Journal of Materials Chemistry C

Polarity-induced dual room-temperature phosphorescence involving the T_2 states of pure organic phosphors

Journal:	*Journal of Materials Chemistry C*
Manuscript ID	TC-ART-05-2022-002152.R2
Article Type:	Paper
Date Submitted by the Author:	03-Sep-2022
Complete List of Authors:	Zang, Lixin; University of Michigan; Shandong Normal University, College of Chemistry, Chemical Engineering and Materials Science Shao, Wenhao; University of Michigan, Chemistry; University of Michigan Bolton, Onas ; University of Michigan Ansari, Ramin; University of Michigan, Department of Chemical Engineering Yoon, Seong-Jun; University of Michigan Heo, Jung-Moo; University of Michigan Kieffer, John; University of Michigan, Materials Science and Engineering; University of Michigan, Matzger, Adam; University of Michigan, Chemistry Kim, Jinsang; University of Michigan, Materials Science and Engineering

ARTICLE

Polarity-induced dual room-temperature phosphorescence involving the T_2 states of pure organic phosphors

Received 00th January 20xx,
Accepted 00th January 20xx

DOI: 10.1039/x0xx00000x

Lixin Zang,[a,b] Wenhao Shao,[c] Onas Bolton,[a] Ramin Ansari,[d] Seong Jun Yoon,[a] Jung-Moo Heo,[a] John Kieffer,[a] Adam J. Matzger[c,e] and Jinsang Kim[a,c,d,e]*

Emissions from higher excited states are of theoretical and experimental interest but rare. A series of pure organic phosphors, 2,5-dihexyloxy-4-bromobenzaldehyde (Br6A) derivatives, show intriguing dual-phosphorescence characteristics. Their phosphorescence emissions are blue-shifted by 20 nm at room temperature compared to those at 78 K. These shifts are accompanied by increasing contributions from a fast-decaying component. The mechanism responsible for the emission shifts observed for Br6A was studied in a 2,5-dihexyloxy-4-bromobenzene (Br6) solid matrix and solvents of various polarities. While the decay curve for Br6A in the Br6 matrix showed a single slow process, pure Br6A exhibited an additional faster decay. We demonstrated that the faster decay of pure Br6A arises from the T_2 state, while Br6A in the Br6 matrix emits solely from T_1. Compared to the T_1 state (π,π^*), the n,π^* character of the T_2 state ensures more efficient spin-orbit coupling with the ground state, which facilitates faster decay. The larger polarity of Br6A compared to that of Br6 leads to a lower T_2 level and a smaller T_2-T_1 energy gap in pure Br6A, but not when in the Br6 solid matrix, which enables a T_1 to T_2 thermal population shift in pure Br6A at room temperature. Consistently, the emissions from the Br6A solutions gradually red-shifted with increasing solvent polarity at 78 K. Moreover, the decay curves of Br6A in solvents of low polarity were single-exponential unlike the double-exponential ones observed in polar solvents. These results provide insight into the effect of the environment on the dual phosphorescence emissions of pure organic phosphors.

Introduction

Phosphorescence typically originates from the lowest triplet excited state (T_1) based on Kasha's rule[1,2] due to photonic energy losses through internal conversion and vibrational relaxation. Even though this rule applies to most emissive organic molecules, some exceptions, in which emissions occur from higher excited states, are of theoretical and experimental interest.[3] Examples of organic molecules that exhibit T_2 phosphorescence include aromatic carbonyl compounds, quinones, and halogenated aromatic compounds.[4] Violating Kasha's rule is realized when intersystem crossing from S_1 to T_2 is fast and the energy gap between T_2 and T_1 is very large or the moieties bearing the T_2 and T_1 states are spatially separated.[5,6] Consequently, achieving emission from a higher level is important for practical applications that include dual emissions from a single molecule. Interestingly, dual phosphorescence emissions from both the T_1 and T_2 states of a single organic molecule has been reported to form white light at room temperature.[7] Very recently, an interesting temperature-dependent dual phosphorescence emission due to thermally activated excitonic coupling between conformers having different dihedral angles was also reported.[8] However, emissions from higher triplet excited states are still scarce and the mechanism for inducing T_2 phosphorescence is not fully understood.

Nevertheless, phosphorescence from the upper T_2 state can occur by two routes. One is not involving the lower triplet state T_1 and the other is thermally populated from T_1.[5,7] When it comes to the second route, the occurrence of T_2 phosphorescence has been attributed to the close proximity of the T_2 state to the T_1 state, with T_2 having a much higher oscillator strength than T_1.[9] However, how to practically decrease the energy gap between T_2 and T_1 to induce T_2 phosphorescence remains unclear. In particular, the effect of environment on the T_2 and T_1 energy levels has not been investigated.

In this study, we found that the emissions from a series of pure organic phosphors shifted hypsochromically at room temperature compared to at 78 K. A plausible mechanism for

[a] Department of Materials Science and Engineering, University of Michigan, Ann Arbor, MI 48109, United States.
[b] College of Chemistry, Chemical Engineering and Materials Science, Shandong Normal University, Ji'nan, 250014, China.
[c] Department of Chemistry, University of Michigan, Ann Arbor, MI 48109, United States.
[d] Department of Chemical Engineering, University of Michigan, Ann Arbor, MI 48109, United States.
[e] Macromolecular Science and Engineering, University of Michigan, Ann Arbor, MI 48109, United States.
† *Corresponding Author: Jinsang@umich.edu

Electronic Supplementary Information (ESI) available: Decay curves for Br6A at room temperature and 78 K, emission spectra of molten Br6A at different temperatures, chemical structure of Br6, the ratio between the rate constant of the faster decay and that of the slower decay. See DOI: 10.1039/x0xx00000x

this shift is proposed based on dual phosphorescence emissions from T_2 and T_1. The thermally activated T_2 phosphorescence was found to be induced by the polarity of the environment. The influence of solid matrixes with various polarities on the emission spectra was studied. Emission spectra and emission decay curves were also investigated in solvents with different polarities. Other possible mechanisms were excluded by means of thorough analyses based on XRD, excitation spectroscopy, and emission decay curves at various concentrations. The results consistently led us to conclude that the polarity of the environment is the determining factor of the occurrence of room temperature phosphorescence (RTP) from T_2 with charge-transfer character.

Experimental

Materials

All reagents were purchased from Sigma-Aldrich and used as purchased without further purification. Deuterated solvents for nuclear magnetic resonance (NMR) spectroscopy were purchased from Cambridge Isotope Laboratories.

Sample preparation

2,5-Dihexyloxy-4-bromobenzene (Br6), 2,5-dihexyloxy-4-chlorobenzaldehyde (Cl6A), 2,5-dihexyloxy-4-bromobenzaldehyde (Br6A), and 2,5-dihexyloxy-4-iodobenzaldehyde (I6A) were synthesized following the procedures reported in our previous publication.[10] Fast-cooled melted powder samples were obtained by melting the crystalline powder samples, followed by rapid cooling in liquid nitrogen to suppress crystal formation. Powder samples with different Br6A concentrations in Br6 matrix (2 wt%, 10 wt%, 50 wt%, and 100 wt%) were prepared by melt-blending Br6A and Br6 at 80 °C, followed by rapid cooling in liquid nitrogen.

Measurements

Photoluminescence emission spectra were collected using a Photon Technologies International (PTI) Quanta Master instrument equipped with an integrating sphere. Gated emission and phosphorescence lifetime data were collected using a PTI Laser Strobe instrument equipped with a Xenoflash lamp. Samples were excited by a 365 nm hand-held UV lamp and photographic images were captured using a digital camera (Nikon D7100).

For experiments at different temperatures, samples were placed on a heating stage in a vacuum chamber. Liquid nitrogen was used to cool the heating stage. The temperature of the heating stage was monitored and controlled from 295 to 78 K using Agilent equipment with an error of ± 0.03 K.

The quantum yield of triplet state formation Φ_T and intersystem crossing rate constant K_{ISC} of Br6A at room temperature were obtained based on the following equation reported in a published study.[11]

$$\Phi_T = \Phi_P \tau_P' \Phi_T' / \Phi_P' \tau_P = K_{ISC} \tau_F, \quad (1)$$

where Φ_P is the phosphorescence quantum yield at room temperature; τ_P is the phosphorescence lifetime at room temperature; Φ_P' and τ_P' are the phosphorescence quantum yield and lifetime, respectively, at 78 K; Φ_T' is the quantum yield of triplet state formation at 78 K; and τ_F is fluorescence quantum yield at room temperature.

Quantum chemical calculations

Geometry optimization and vertical excitation energy calculations for Br6A were carried out by means of density functional theory (DFT) and time-dependent density functional theory (TD-DFT) calculations, implemented in the Gaussian 09 package using the B3LYP functional and the 6-31g(d,p) basis set in a vacuum. Spin-orbit coupling (SOC) was studied in the Dalton 2016[12] package using the B3LYP functional and the cc-pVDZ basis set[13] in a vacuum based on the ground-state geometry optimized in Gaussian 09.

Results and discussion

Red-shifted phosphorescence at low temperature

Figure 1a shows the molecular structures of the organic phosphors studied in this work, including Cl6A, Br6A, and I6A. In the solid state, they efficiently emit green RTP at approximately 500 nm (**Figures 1b-d**). Molecular features that enable RTP with millisecond lifetimes[14] are: (1) aldehyde groups bearing low-energy n,π* states that create n,π* to π,π* channels (**Figure 1a**) for efficient intersystem crossing (ISC), according to El-Sayed rules,[15] and (2) the heavy atom (Cl, Br, and I) effect[16] that enhances SOC efficiency. For instance, the difference in the electronic configuration and small energy gap between the S_1 (n,π*) and T_3 (π,π*) energy states enable efficient ISC from S_1 to T_3 (**Figure 1a**).

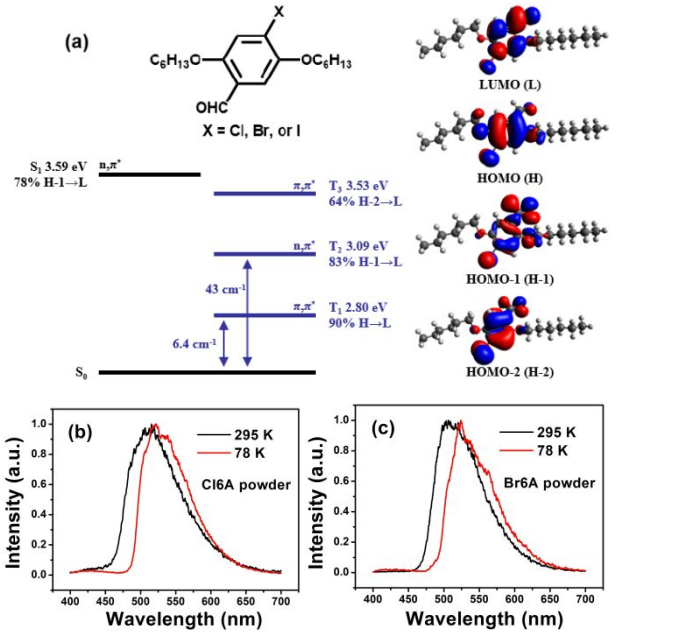

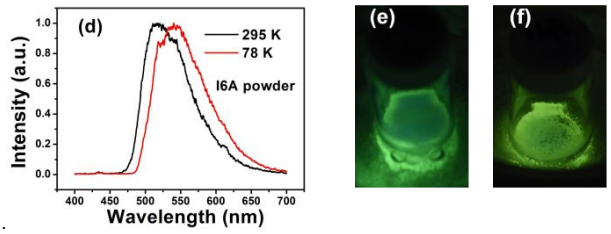

Figure 1. (a) Molecular structures of emitters studied in this work, including Cl6A, Br6A, and I6A; energy state diagram and major contributing molecular orbitals of Br6A in vacuum (arrows indicate the spin-orbit coupling matrix element (SOCME) between triplet energy states and the ground state). (b-d) Time-resolved emission spectra (with a delay time of 300 μs) of their crystalline powders at room temperature and at 78 K. Emission of the Br6A powder excited at 365 nm in a glass vial (e) right after transferring from room temperature to liquid nitrogen and (f) after being stabilized at liquid nitrogen temperature for one minute.

The phosphorescence emission spectra (**Figures 1b-d**) show that all three compounds undergo approximately 20 nm hypsochromic shifts upon heating from 78 K to 295 K. **Figures 1e** and 1**f** show that the emission of the Br6A powder changed from bluish-green to yellowish-green upon cooling from room temperature to liquid nitrogen temperature, consistent with the results obtained from the emission spectra shown in **Figures 1b-d**.

To investigate the nature of the emission shift in detail, the phosphorescence spectra of the Br6A crystalline powder were recorded at various temperatures from 295 K to 78 K (**Figure 2a**). The emission λ_{max} decreased with increasing temperature, while two split peaks were distinctly observed at 185 K and 130 K. The correlation between the peak wavelength and temperature is plotted in the inset of **Figure 2a**. Interestingly, the phosphorescence intensity was observed to decrease from 295 to 105 K, followed by an increase from 105 to 78 K (**Figure 2b**). Thermally activated quenching of the green phosphorescence and simultaneous enhancement of the yellow phosphorescence were observed as the temperature was lowered.

Two decay components can be extracted from the decay curves of the Br6A crystalline powder at various temperatures (**Figure 2c**). The faster component is approximately 4–7 times faster than the slower component (**Table 1**). **Figure 2d** shows the portion of the slower and faster decay components as functions of temperatures. The contribution of the faster decay component increased from 20% at 78 K to 69% at 295 K. The gradual increase in the fast-decay component with increasing temperature (**Figure 2d** and **Table 1**) implies that this faster decaying phosphorescence originates from thermally activated T_2 excitons, similar to that previously reported by Tang *et al.*[7]

The value of Φ_P for Br6A is 2.9%, as we previously reported.[17] At 78 K, non-radiative decay and quenching can be neglected, and hence Φ_P' was assumed to be equal to Φ_T'. In addition, τ_P' and τ_P can be determined based on the data shown in Fig. 2c. Accordingly, the value of Φ_T was obtained as 35.2%. τ_F for Br6A was reported to be 0.5 ns.[17] K_{ISC} was then calculated to be 7.04×10^8 s^{-1}, which is quite fast as the result of the heavy atom effect of bromine.

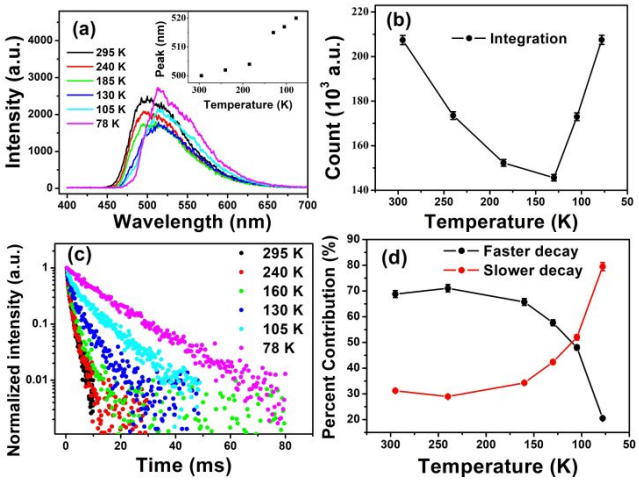

Figure 2. (a) Phosphorescence emissions of the Br6A crystalline powder at various temperatures from 295 K to 78 K. Inset: correlation between the emission λ_{max} and temperature. For the spectra at 185 K and 130 K, the average values of the two emission peaks are used. (b) The integration area of the phosphorescence emission at different temperatures. (c) Decay of the Br6A crystalline powder emissions monitored at 500 nm at different temperatures. (d) ($A_1/(A_1+A_2)$ and $A_2/(A_1+A_2)$) of the longer (A_1) and shorter lifetime (A_2) components as functions of temperature.

Table 1. Lifetimes and contributions of the two decay components at various temperatures fitted by double-exponential decay functions

Temperature (K)	τ_1 (ms)	τ_2 (ms)	A_1 (%)	A_2 (%)
295	1.97	0.54	31.2	68.8
240	2.09	0.51	29.2	70.8
185	2.83	0.58	34.5	65.5
130	4.60	0.72	42.7	57.3
105	8.88	1.37	52.3	47.7
78	14.2	3.34	79.8	20.2

To understand the contribution of the two decay components to the emission profile, we studied the emissions with different delay times at 105 K, where the two decay components make approximately equal contributions. The spectrum red-shifted with increasing delay time (**Figure 3a**), which indicates that the emission with the longer wavelength is the slower component. Furthermore, the contribution of the faster decay component decreased with increasing wavelength (**Figure 3b**). These results are consistent throughout the crystalline powder (**Figure 3a**), fast-cooled melted powder (**Figure S1**), and single crystals (**Figure 3b**), which indicates that the phosphorescence of Br6A is derived from two emissive states. Thermal repopulation from T_1 to T_2 is plausibly responsible for the emergence of the fast-decaying component with increasing temperature at the higher-energy side of the phosphorescence emission. Compared to the T_1 state (π–π^*), the n-π^* nature of the T_2 state ensures more efficient spin-orbit coupling with the ground state, which results in faster decay.

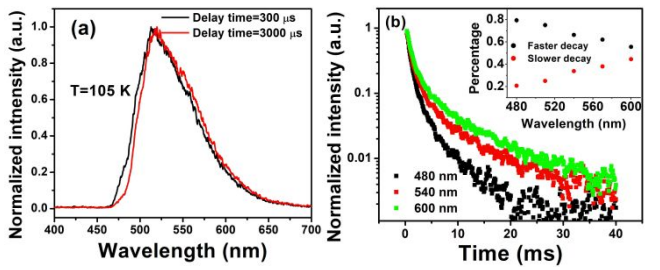

Figure 3. (a) Phosphorescence emission spectra of the Br6A crystalline powder with decay times of 300 and 3000 μs at 105 K. (b) Phosphorescence decay of the single crystal of Br6A at 130 K monitored at different wavelengths. Inset: Percent contributions of the faster and slower decay components fitted from the decay curves monitored at different wavelengths.

Debunking ground-state aggregation and the existence of excimers

In addition to thermally activated T_2 phosphorescence, other mechanisms, such as ground-state aggregation or the presence of excimers, can also shift emissions. Typical types of ground-state aggregation involve J- and H-aggregates that exhibit hypsochromically or bathochromically shifted emissions, respectively,[18] which were originally developed by Kasha *et al.* to treat aggregates of small molecules. Raising the temperature may change the distance between adjacent Br6A molecules and the degree of aggregation, potentially shifting the emission and giving rise to new decay components. **Figure 4a** shows the variable-temperature X-ray diffraction (XRD) results for Br6A. While the (2,0,2) peak shows a small gradual shift to larger angles as temperature decreased, a much insignificant shift to smaller angles was observed in the (1,0,0) peak, indicating minor uniaxial lattice stretching. However, the observed minimal change confirms that ground-state aggregation did not occur because ground-state aggregation would have induced a significant change in the XRD pattern. In addition, the phosphorescence excitation profile of the fast-cooled melt-blended Br6A-Br6 solid solution (chemical structure of Br6 in Figure S2) at various concentrations (Br6 has limited absorption at the excitation wavelength (365 nm) used in this work and does not emit at room temperature) exhibited minimal change in spectral shape and peak position (**Figure 4b**), which suggests that the ground-state aggregation of Br6A is unlikely.

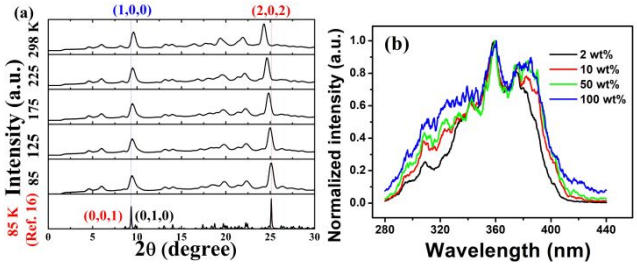

Figure 4. (a) Temperature-variant XRD spectra of the Br6A crystalline powder with reference to the simulated powder XRD profile from single-crystal XRD.[17] Assignments of major peaks are provided. (b) Normalized excitation spectra for different concentrations of Br6A in the Br6 matrix.

Alternatively, the existence of an excimer may induce a secondary decay component. When the excited molecule strongly interacts with an adjacent ground-state molecule, the formation of the excimer state lowers the energy of the original excited state, which normally undergoes slower decay due to the additional process required for the formation of the excimer.[19,20] Figure5 shows low-temperature decay curves for Br6A in the Br6A-Br6 solid-solution at various concentrations monitored at various emission wavelengths. Table 2 shows the fitted lifetime data for Br6A in the Br6A-Br6 solid-solution at various concentrations monitored at various emission wavelengths corresponding to Figure 5. With increasing concentration of Br6A in the melt-blended Br6A-Br6 solid solution, We observed a gradual emergence of the fast lifetime component indicated by the increase of A_2 at the higher-energy side of the emission (from 630 to 480 nm) instead of the slower decay, which does not conform to the excimer principle.

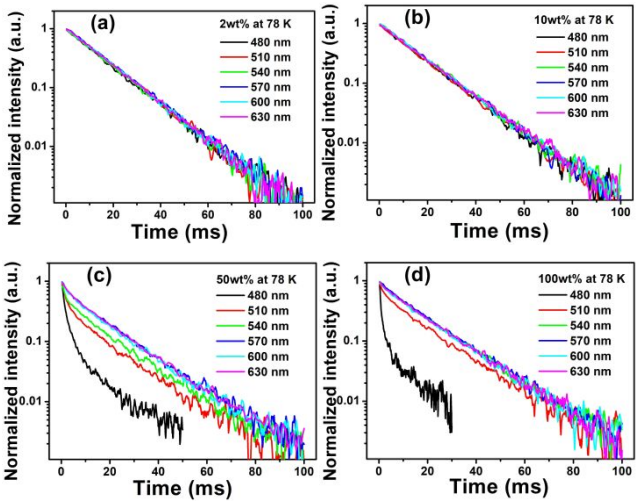

Figure 5. Low-temperature decay curves for Br6A in the Br6A-Br6 solid-solution at various concentrations monitored at various emission wavelengths.

Table 2. Fitted lifetime data for the phosphorescence of Br6A in the Br6A–Br6 solid-solution at various concentrations, monitored at various emission wavelengths

Br6A concentration	Fit parameter	Emission wavelength 480 nm	510 nm	540 nm	570 nm	600 nm	630 nm
2%	τ (ms)	13.2	14.2	14.2	13.9	14.1	13.7
10%	τ (ms)	13.3	13.9	14.0	14.2	14.1	14.3
50%	τ_1 (ms)	6.00	13.5	13.9	15.0	14.8	15.3
	τ_2 (ms)	1.02	1.60	1.34	1.90	2.30	2.83
	A_1 (%)	19.3	37.8	53.2	68.9	67.5	69.9
	A_2 (%)	80.7	62.2	46.8	31.1	32.5	30.1
100%	τ_1 (ms)	4.10	14.9	15.9	15.9	15.6	15.3
	τ_2 (ms)	0.46	1.78	2.43	3.98	2.05	1.47
	A_1 (%)	12.8	66.0	80.1	86.5	84.1	84.9
	A_2 (%)	87.2	34.0	19.9	13.5	15.9	15.1

Theoretical evidence for thermally activated dual phosphorescence

Thermally activated phosphorescence from a higher triplet state (T_n) requires a small energy gap between the T_n and T_1 states, besides a high radiative decay rate. To gain deeper insight into our system, we used DFT and its time-dependent form (TD-DFT) to study the energy states of Br6A and the spin-orbit coupling matrix elements (SOCMEs) between the ground state and triplet excited states (the observed radiative decay rate is proportional to the SOCME square term). The computational results (**Figure 1a**) indicate that the energy gap between T_2 and T_1 (0.28 eV) is small enough to thermally populate T_2, which is experimentally supported by the phosphorescence emission energy difference in the Br6A crystalline power at 78 and 295 K (**Figure 1c**). In addition, analysis of the major frontier molecular orbitals contributing to the T_1 and T_2 states shows that the T_2 state has strong n-π* character due to the contribution of the non-bonding electrons of the aldehyde group to the HOMO-1 orbital, while T_1 has π–π* character (**Figure 1a**). This difference induces a much larger SOCME between the T_2 and S_0 states than the T_1 and S_0 states. Meanwhile, the experimental decay rate constant for the T_2 state (see **Figure S4**) is 4–7 times higher than that of T_1 over the entire temperature range (78–295 K). These results suggest that Br6A satisfies the requirements for thermally activated dual phosphorescence.

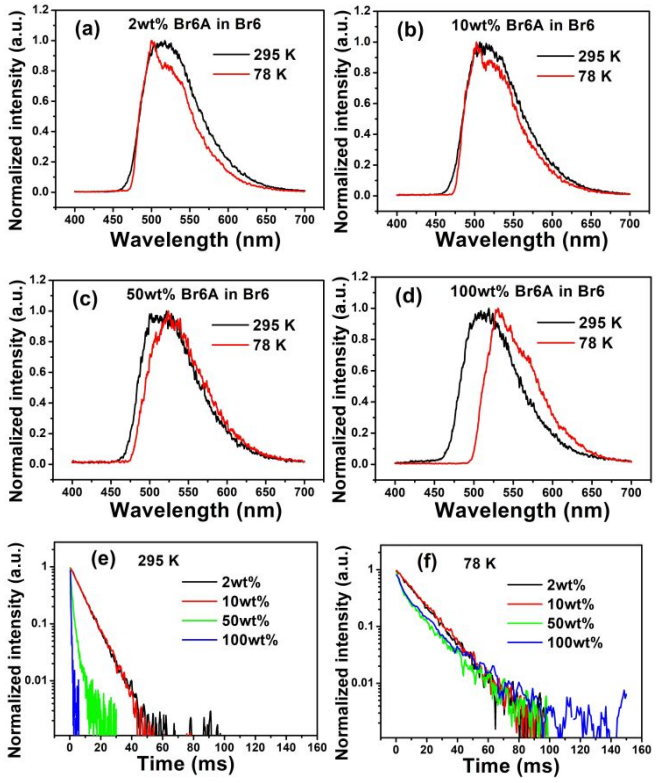

Figure 6. (a-d) Phosphorescence spectra of Br6A in Br6 with different concentrations at room temperature and 78 K. (e) Decay curves monitored at 500 nm of Br6A in the Br6A-Br6 solid-solution at various concentrations at room temperature. (f) Decay curves monitored at 500 nm of Br6A in the Br6A-Br6 solid-solution at various concentrations at 78 K.

Thermally activated dual phosphorescence induced by polarity

Interestingly, we found that the melt-blended Br6A-Br6 solid solution system exhibited a gradual increase in the hypsochromic shift from 78 K to 295 K, as the concentration of Br6A increased (**Figures 6a-d**). **Figures 6e and 6f** shows the decay curves for Br6A at different concentrations at room temperature and 78 K. Table 3 shows the fitted lifetime data of Br6A in the Br6A-Br6 solid-solution at various concentrations at room temperature and 78 K. At room temperature, the decay curve of Br6A at a lower concentration in the Br6A-Br6 solid solution (lower than 10 wt%) is single-exponential, while the decay curve of the more-concentrated Br6A sample (50 and 100 wt%) is double-exponential. Furthermore, the lifetime of the diluted sample is similar to that of the slow component of the concentrated sample. **Figure 6f** shows the decay curves of Br6A at different concentrations at 78 K. The decay curve of the diluted sample remained single-exponential with minimal change (but became slightly slower) compared to that at room temperature. Meanwhile, the slow component in the decay curve of the more-concentrated samples becomes more dominated at 78 K. Thus, Br6A shows a temperature-independent single emission at lower concentration, while the concentrated Br6A sample shows two emissions that are temperature-dependent.

Table 3. Fitted lifetime data for Br6A in the Br6A–Br6 solid-solution at various concentrations, at room temperature and 78 K

T (K)	Fit parameter	Solid-solution concentration 2 wt%	10 wt%	50 wt%	100 wt%
295	τ_1 (ms)	7.60	7.70	2.18	1.17
	τ_2 (ms)	-	-	0.65	0.27
	A_1 (%)	100	100	84.6	25.0
	A_2 (%)			15.4	75.0
78	τ_1 (ms)	13.3	13.8	14.1	16.6
	τ_2 (ms)	-	-	2.23	3.37
	A_1 (%)	100	100	49.3	50.7
	A_2 (%)	-	-	50.7	49.3

Comparing the RTP data for the 2 wt% Br6A-Br6 solid solution (only T_1 emission, **Figure 6a, black line**) with that of pure Br6A (T_1 & T_2 emission, **Figure 6d, black line**) reveals that the former is bathochromically shifted by about 8 nm (**Figure 7**). Notwithstanding this small shift, their emission lifetimes differ significantly (**Figure 6e**). The decay curve for Br6A comprises a faster decay (T_2) and a slower decay (T_1), while the decay curve for 2 wt% Br6A in Br6 only shows the slower decay (T_1), which indicates that no thermal repopulation occurs in 2 wt% Br6A in Br6 because the energy gap is not small enough. The thermal repopulation observed for pure Br6A is promoted by the small energy gap induced by the higher polarity of Br6A.

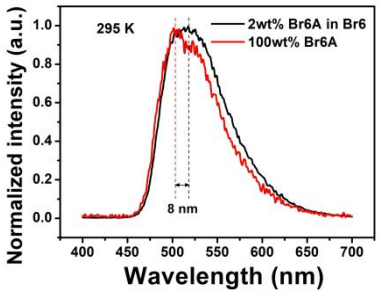

Figure 7. Comparison between the emission spectra of 2 wt% Br6A-Br6 and pure Br6A.

Based on the thermally activated dual phosphorescence mechanism established for the Br6A-related systems, we conclude that, the T_2 phosphorescence contribution is gradually induced by increasing the concentration of Br6A in the Br6A-Br6 solid solution. The higher polarity of Br6A compared to that of Br6 implies possible T_2 phosphorescence of Br6A in polar environments. This hypothesis is supported by molecular orbital analysis (**Figure 1a**), which shows that the T_2 state has charge-transfer character due to its n,π* nature, while the T_1 state is more localized on the phenyl core. According to the Frank–Condon principle, the energy levels of the T_2 and T_1 states can be lowered by solvent relaxation prior to radiative decay,[21] and the charge-transfer character of the former results in a larger reduction in polar environments. Consequently, thermally populated dual phosphorescence is more effectively activated in polar environments due to the reduced T_1-T_2 energy gap.

Emission of Br6A in solvents with different polarities

To investigate whether or not dual phosphorescence can be induced in a polar environment, we analyzed the phosphorescence emission profiles of a diluted Br6A solution in solvents with varying polarities at 78 K (**Figure 8a**). The occurrence of fast phosphorescence decay gradually increased as the solvent polarity was increased from toluene to acetonitrile (**Figure 8b**), and its contribution to the total phosphorescence emission reached 53.5% (**Table 4**) in acetonitrile. The decay curves for Br6A in the lower-polarity solvents (toluene and tetrahydrofuran, THF) are single-exponential, while those in the higher-polarity solvents (acetone and acetonitrile) are double-exponential, which indicates the Br6A emission in toluene or THF arises from a single energy state, while that in acetone or acetonitrile arises from two energy states.

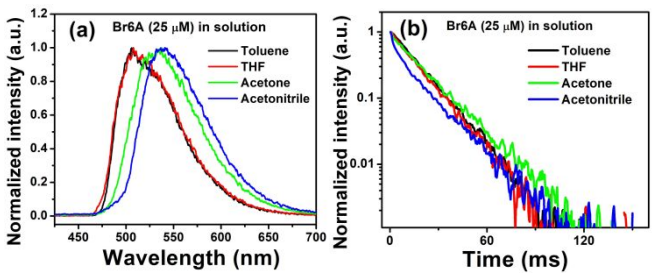

Figure 8. (a) Emission spectra and (b) decay curves monitored at 500 nm for Br6A in toluene, THF, acetone, and acetonitrile at 78 K.

Explaining the studied systems based on the proposed mechanism

Figure 9 presents a schematic of the emission properties of Br6A under various experimental conditions of varying polarity. The dual phosphorescence profile of Br6A is regulated by the polarity of the environment and available thermal energy: 1) T_2 phosphorescence can be thermally activated through the up-conversion from T_1 excitons when the T_2-T_1 energy gap is sufficiently small; 2) emission arises only from the T_1 state in a low-polarity environment due to the relatively large T_2-T_1 energy gap that blocks the thermal population pathway, whereas a high polarity environment reduces the T_2-T_1 energy gap, thereby enabling T_2 phosphorescence with the available thermal energy.

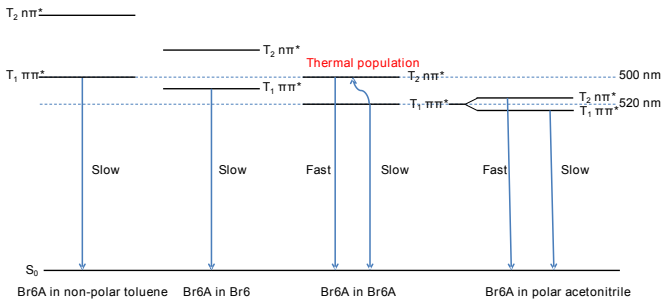

Figure 9. Illustrating the emission properties of Br6A in different polarity environments based on the proposed dual phosphorescence emission mechanism. Br6A is a more polar molecule than Br6.

Table 4. Lifetimes and percentage contributions of the short and long decay components of Br6A in various solvents fitted by double-exponential decay functions

Solvent	τ_1 (ms)	τ_2 (ms)	A_1 (%)	A_2 (%)
Toluene	15.1	-	100	0.0
THF	14.2	-	100	0.0
Acetone	17.2	0.792	77.5	22.5
Acetonitrile	13.9	0.939	46.5	53.5

Conclusions

The phosphorescence emissions from Cl6A, Br6A, and I6A, a series of pure organic phosphors, show dual phosphorescence emissions from T_1 and thermally activated T_2 that depend on the experimental temperature and the polarity of the environment. Hypsochromic shifts were observed as the temperature was increased from 78 to 295 K; these shifts are accompanied by increasing contributions from short-lifetime components. The environmental polarity of the organic phosphor was revealed to be the key to inducing the occurrence of the T_2 emission because a polar environment reduces the energy gap between T_2, with charge-transfer character, and the T_1 state, which facilitates thermal population of the T_2 state. The presented findings provide insight into phosphorescence from higher energy states, as

well as feasible rational T_2 phosphor and dual phosphoresce emitter designs.

Author Contributions

Lixin Zang: Conceptualization, Investigation, Writing—Original draft preparation; **Wenhao Shao**: Investigation, Calculation; **Onas Bolton**: Methodology, Investigation; **Ramin Ansari**: Visualization, Calculation; **Seong Jun Yoon, Jung-Moo Heo**: Data curation, Formal analysis; **John Kieffer**: Supervision of calculations; **Adam J. Matzger**: Conceptualization, Data curation, Formal analysis; **Jinsang Kim**: Conceptualization, Project administration, Writing—Reviewing and Editing, Funding acquisition.

Conflicts of interest

There are no conflicts to declare.

Acknowledgment

We acknowledge financial support from the "Designing Materials to Revolutionize and Engineer our Future (DMREF)" program of the Division of Materials Research (DMR) of the National Science Foundation (NSF) (grant number: 143965). This work was also partly supported by the Qatar National Research Fund (grant number: NRPP8-245-1-059). We also acknowledge a fellowship for L. X. Zang from the National Natural Science Foundation of China (grant number: 61905132).

References

1. L. Paul, S. Chakrabarti and K. Ruud, Anomalous phosphorescence from an organometallic white-light phosphor. *J. Phys. Chem. Lett.*, 2017, **8**(19), 4893.

2. Y. Xu, P. Xu, D. Hu and Y. Ma, Recent progress in hot exciton materials for organic light-emitting diodes. *Chem. Soc. Rev.*, 2021, **50**(2), 1030.

3. H. Wang, J. Wang, T. Zhang, Z. Xie, X. Zhang, H. Sun, Y. Xiao, T. Yu and W. Huang, Breaching kasha's rule for dual emission: Mechanisms, materials and applications. *Journal of Materials Chemistry C*, 2021.

4. T. Itoh, Fluorescence and phosphorescence from higher excited states of organic molecules. *Chem. Rev.*, 2012, **112**(8), 4541.

5. C. Feng, S. Li, L. Fu, X. Xiao, Z. Xu, Q. Liao, Y. Wu, J. Yao and H. Fu, Breaking kasha's rule as a mechanism for solution-phase room-temperature phosphorescence from high-lying triplet excited state. *J. Phys. Chem. Lett.*, 2020, **11**(19), 8246.

6. L. Paul, T. Moitra, K. Ruud and S. Chakrabarti, Strong duschinsky mixing induced breakdown of kasha's rule in an organic phosphor. *J. Phys. Chem. Lett.*, 2019, **10**(3), 369.

7. Z. He, W. Zhao, J. W. Y. Lam, Q. Peng, H. Ma, G. Liang, Z. Shuai and B. Z. Tang, White light emission from a single organic molecule with dual phosphorescence at room temperature. *Nat Commun*, 2017, **8**(1), 416.

8. T. Wang, J. De, S. Wu, A. K. Gupta and E. Zysman-Colman, Thermally activated and aggregation-regulated excitonic coupling enable emissive high-lying triplet excitons. *Angew. Chem. Int. Ed. Engl.*, 2022, e202206681.

9. T. Itoh, Phosphorescence from the t2(n, π∗) state observed for 4-hyroxybenzaldehyde in a p-dichlorobenzene matrix. *Chem. Phys. Lett.*, 2014, **591**, 109.

10. L. Zang, W. Shao, M. S. Kwon, Z. Zhang and J. Kim, Photoresponsive luminescence switching of metal‐free organic phosphors doped polymer matrices. *Advanced Optical Materials*, 2020, **8**(23), 2000654.

11. S. M. Ramasamy and R. J. Hurtubise, Room-temperature luminescence properties of p -aminobenzoic acid adsorbed on sodium acetate-sodium chloride mixtures. *Anal. Chem*, 1987, **59**, 2144.

12. K. Aidas, C. Angeli, K. L. Bak, V. Bakken, R. Bast, L. Boman, O. Christiansen, R. Cimiraglia, S. Coriani, P. Dahle, E. K. Dalskov, U. Ekstrom, T. Enevoldsen, J. J. Eriksen, P. Ettenhuber, B. Fernandez, L. Ferrighi, H. Fliegl, L. Frediani, K. Hald, A. Halkier, C. Hattig, H. Heiberg, T. Helgaker, A. C. Hennum, H. Hettema, E. Hjertenaes, S. Host, I. M. Hoyvik, M. F. Iozzi, B. Jansik, H. J. Jensen, D. Jonsson, P. Jorgensen, J. Kauczor, S. Kirpekar, T. Kjaergaard, W. Klopper, S. Knecht, R. Kobayashi, H. Koch, J. Kongsted, A. Krapp, K. Kristensen, A. Ligabue, O. B. Lutnaes, J. I. Melo, K. V. Mikkelsen, R. H. Myhre, C. Neiss, C. B. Nielsen, P. Norman, J. Olsen, J. M. Olsen, A. Osted, M. J. Packer, F. Pawlowski, T. B. Pedersen, P. F. Provasi, S. Reine, Z. Rinkevicius, T. A. Ruden, K. Ruud, V. V. Rybkin, P. Salek, C. C. Samson, A. S. de Meras, T. Saue, S. P. Sauer, B. Schimmelpfennig, K. Sneskov, A. H. Steindal, K. O. Sylvester-Hvid, P. R. Taylor, A. M. Teale, E. I. Tellgren, D. P. Tew, A. J. Thorvaldsen, L. Thogersen, O. Vahtras, M. A. Watson, D. J. Wilson, M. Ziolkowski and H. Agren, The dalton quantum chemistry program system. *Wiley Interdiscip Rev Comput Mol Sci*, 2014, **4**(3), 269.

13. T. H. Dunning, Gaussian basis sets for use in correlated molecular calculations. I. The atoms boron through neon and hydrogen. *The Journal of Chemical Physics*, 1989, **90**(2), 1007.

14. O. Bolton, D. Lee, J. Jung and J. Kim, Tuning the photophysical properties of metal-free room temperature organic phosphors via compositional variations in bromobenzaldehyde/dibromobenzene mixed crystals. *Chem. Mater.*, 2014, **26**(22), 6644.

15. S. Hirata, Recent advances in materials with room-temperature phosphorescence: Photophysics for triplet exciton stabilization. *Advanced Optical Materials*, 2017, **5**(17).

16. J. Yang, X. Zhen, B. Wang, X. Gao, Z. Ren, J. Wang, Y. Xie, J. Li, Q. Peng, K. Pu and Z. Li, The influence of the molecular packing on the room temperature phosphorescence of purely organic luminogens. *Nat Commun*, 2018, **9**(1), 840.

17. O. Bolton, K. Lee, H. J. Kim, K. Y. Lin and J. Kim, Activating efficient phosphorescence from purely organic materials by crystal design. *Nat. Chem.*, 2011, **3**(3), 205.

18. Y. Deng, W. Yuan, Z. Jia and G. Liu, H- and j-aggregation of fluorene-based chromophores. *J. Phys. Chem. B*, 2014, **118**(49), 14536.

19. M. Son, K. H. Park, C. Shao, F. Wurthner and D. Kim, Spectroscopic demonstration of exciton dynamics and excimer formation in a sterically controlled perylene bisimide dimer aggregate. *J. Phys. Chem. Lett.*, 2014, **5**(20), 3601.

20. H. Osaki, C. M. Chou, M. Taki, K. Welke, D. Yokogawa, S. Irle, Y. Sato, T. Higashiyama, S. Saito, A. Fukazawa and S. Yamaguchi, A macrocyclic fluorophore dimer with flexible linkers: Bright excimer emission with a long fluorescence lifetime. *Angew. Chem. Int. Ed. Engl.*, 2016, **55**(25), 7131.

21. V. Karunakaran and S. Das, Direct observation of cascade of photoinduced ultrafast intramolecular charge transfer dynamics in diphenyl acetylene derivatives: Via solvation and intramolecular relaxation. *J. Phys. Chem. B*, 2016, **120**(28), 7016.